The effect of humeral implant thickness and canal fill on interface contact and bone stresses in the proximal humerus

Stephanie Synnott, MESc, G. Daniel G. Langohr, PhD, Jacob M. Reeves, PhD, James A. Johnson, PhD, George S. Athwal, MD, FRCSC*

Roth|McFarlane Hand and Upper Limb Center Biomechanics Laboratory, London, ON, Canada

ARTICLE INFO

Background: Stem size is an important element for successful time zero primary fixation of a press-fit humeral stem in shoulder arthroplasty. Little basic science research, however, has been conducted on the effects of implant thickness and canal fill on load transfer, contact, and stress shielding. The purpose of this finite element study was to determine the effects of varying stem thickness on bone contact, bone stresses, and bone resorption owing to stress shielding.

Methods: Three generic short-stem implant models were developed and varied based on cross-sectional thickness (thinner − 8 mm, medium − 12 mm, thicker − 16 mm). Using a finite element model, three outcome measures were determined (1) the amount of bone-to-implant contact, (2) changes in cortical and trabecular bone stresses from the intact state, and (3) changes in cortical and trabecular strain energy densities which can predict bone remodeling or stress shielding.

Results: Increasing the size of the humeral stem had no significant effects on bone-to-implant contact during loading ($P > .07$). The thinner implant with the lowest canal fill ratio produced significantly lower changes in stress from the intact state in both cortical and trabecular bone ($P < .002$). In addition, the thinner implant resulted in a substantially lower volume of bone predicted to stress shield and resorb when compared with the medium and thicker stems.

Discussion: The results demonstrate that thinner implants and lower canal fill may be beneficial over thicker sizes, provided equal initial fixation can be achieved. The thinner implant has a greater degree of load sharing and increases the mechanical load placed on surrounding bone, reducing the risk of stress shielding and bone resorption.

Humeral implants for shoulder arthroplasty have evolved over the years; however, complications such as implant loosening and proximal stress shielding still occur.[5–7,15,24] Some aspects of humeral stem design that have been investigated, in terms of the effect on bone stress and stress shielding, are implant stem length and material stiffness or modulus.[7,23,25,28] However, some aspects of humeral stem design and mode of implantation require further research, such as the effect of implant thickness and canal fill ratio. In a clinical study, Nagels et al[19] investigated the occurrences of stress shielding in the proximal humerus. The relative size of the implant in the humeral canal was measured and correlated with the degree of bone loss. The results showed that humeral implants with a larger relative stem diameter increased the occurrences of stress shielding. This study only investigated radiographic changes in cortical bone and did not examine changes in trabecular bone or the basic science behind these adaptations. In addition, the incidence of stress shielding was correlated with the use of a standard-length humeral stem and not shorter stems.

Raiss et al[21] examined the canal fill ratio of a shorter-stem implant in a clinical study. The authors found increased bony adaptations and stress shielding with higher fill ratios. The authors recommended that fill ratios remain lower than 0.7 for anatomic shoulder arthroplasty and lower than 0.8 for reverse shoulder arthroplasty using the curved humeral stem examined. Although the authors provided guidelines, these threshold values for fill ratios can only really be applied to the particular stem shape and type examined. The identification that stem shape has an influence on bone adaptations independent of length was reported by Denard et al.[8] In their study, two short-stem implants from different manufacturers were examined for bone adaptations and found to have significantly different rates.

To better predict the capacity of bone resorption and stress shielding in orthopedic models, various studies have investigated changes in strain energy density (SED).[1,3,11,12,14,20,26,27] Changes in SED can be measured across several bone sites using finite element (FE) computational analysis, and can be used to predict regions of bone that are likely to resorb when the change in SED is less than the threshold value of 55%.[20] As such, the objective of this FE study was to determine changes in bone-to-implant contact (BIC), cortical and trabecular bone stresses, as well as the changes in cortical and trabecular SED from the intact state when implant thickness was increased within the proximal humerus using a composite short-stem humeral implant. The composite short-stem implant was a design amalgamation of three commercially available short-stem implants. It was hypothesized that the thickest implant would result in the greatest amount of BIC, the greatest changes in cortical and trabecular bone stress from the intact state, as well as the greatest changes in SED; thus, resulting in an increase in the percent volume of cortical and trabecular bone expected to experience stress shielding and resorption.

Materials and methods

Model development

Digital Imaging and Communications in Medicine data from eight osteoarthritic cadaveric shoulder computed tomography scans (all men, left, mean $\pm$ SD of age = 68 $\pm$ 5 years) were processed using Mimics Software Suite (Materialise, Leuven, Belgium). Eight 3-dimensional solid models of the proximal humerus were created with separate regions of cortical bone and trabecular bone created through the combined use of automatic threshold-based segmentation and manual identification of cortical/trabecular bone boundaries. Cortical bone was separated using an applied mask with threshold of 226 Hounsfield units,[22,30] while a trabecular bone mask was created with manual slice-by-slice segmentation. After appropriate cortical/trabecular bone separation, the surface geometries were exported in STL format into SolidWorks (Dassault Systèmes, S.A. , Vélizy, France).

The resulting 3-dimensional cortical and trabecular geometries were further sectioned into head and shaft components. To create the head component, a humeral head cut plane was created by an experienced shoulder arthroplasty surgeon (GSA). This cut plane was also used as a reference to shorten the trabecular bone to a length of 40 mm distal from this surface, as it has been shown that trabecular density greatly diminishes after 20 mm beneath the resection plane.[24]

Three generic short-stem implant models were created using SolidWorks CAD software. Implant dimensions were measured from three commercially available humeral implants: Arthrex Univers Apex, Biomet Comprehensive Mini Stem, and Wright Medical/Tornier Aequalis Ascend Flex. The shape and upper/middle/lower stem dimensions of the three implants were averaged and used to create the generic implant model (distal stem diameter, d = 12 mm, mean canal fill ratio = 0.6). This base model was then scaled to create an implant with a thinner cross section (d = 8 mm, canal fill ratio = 0.4) and a thicker cross section (16 mm, canal fill ratio = 0.8) (Fig. 1). A stem length of 55 mm from the medial aspect of the stem was chosen for all configurations to mimic clinical short-stem implants.

Several humeral head components were also created to ensure each patient obtained the appropriately sized humeral head. Head geometry was created with an aspect ratio of 1.00:0.85 between the radius of the head and height of the head, respectively. These measurements, again, were obtained from head components currently available commercially (Arthrex Univers Apex, Biomet

Comprehensive Mini Stem, Wright Medical/Tornier Aequalis Ascend Flex).

Reference geometries were created in SolidWorks to accurately align the implants into bone and recreate surgical placement. Two reference sites were created for the bone geometry: a central canal axis down the diaphysis termed the "Diaphyseal Axis" and a plane on the cut surface termed the "Humeral Head Resection Plane." For the implant reference locations, each implant was given a central stem axis named the "Implant Axis" as well as a coincident axis centered along the anterior-posterior face referred to as the "Anterior-Posterior Face Axis."Several mates were then applied to ensure the implants were strictly confined in the bone. Diaphyseal and Implant axes were made coincident and the Humeral Head Resection Plane was made parallel to the Anterior-Posterior Face Axis. Finally, the appropriate anatomic head diameter was selected for each specimen by an experienced shoulder surgeon (GSA). The backside of the humeral head was made coincident with the plane on the cut surface and was appropriately positioned, once again, by an experienced shoulder surgeon (GSA). Finally, the humeral head component was combined with the stem of the implant to simulate the clinical scenario. This configuration assumed ideal alignment conditions, which may not precisely replicate the results routinely obtained clinically.

FE modeling

After implant alignment, all bone and implant geometries were exported from SolidWorks and imported into Abaqus v6.14 (Dessault Systèmes Simulia Corp., Providence, RI, USA) in STEP AP214 or ASIC format. To allow for comparisons between the implanted and native state, identical meshes were required for each specimen model. For each humeral implant stem investigated, partitions were created by cutting and reaming the trabecular bone with the desired implant size. These partitions, along with the head components resected in SolidWorks (cortical and trabecular head components), were assembled and merged while maintaining the geometrical lines of the implant allowing for identical mesh generation (Fig. 2). Thus, the intact and reconstructed states resulted in identical humeral geometries allowing for direct element-to-element comparison of changes in bone stress.[20] The bone and implant were then meshed with quadratic tetrahedral elements with a maximum edge length of 2 mm and maximum deviation factor of 0.06 mm.[22]

Cortical bone was assigned material properties with a uniform elastic modulus of E = 20 GPa and Poisson's ratio of v = 0.3.[22] Trabecular bone, being an inhomogeneous structure with nonuniform properties, was assigned varying material properties based on computed tomography attenuation. Properties were applied using a density-modulus equation.[18]

To calculate apparent density, the Digital Imaging and Communications in Medicine data were imported into Mimics, where a linear relationship was applied based on two substances of known densities placed within the scan: SB3 cortical bone (Gammex, Middleton WI, USA; ρ = 1.82 g/cm^3) and water (ρ = 1.00 g/cm^3). From this, variations in density across the computed tomography scan could be derived and determined for trabecular bone.[22] Poisson's ratio was also set to 0.3 for trabecular bone.[22]

Implant models were all assigned titanium material properties (E = 110 GPa, v = 0.3) with the same site-specific frictional characteristics. The under surface of the humeral heads and the distal humeral stems, where the stem became completely cylindrical, was polished (μ = 0.40), and the proximal region of the humeral stems was plasma sprayed (μ = 0.88). Application of these frictional properties was applied to be relatively consistent with the clinical implants that the generic implants were modeled from.
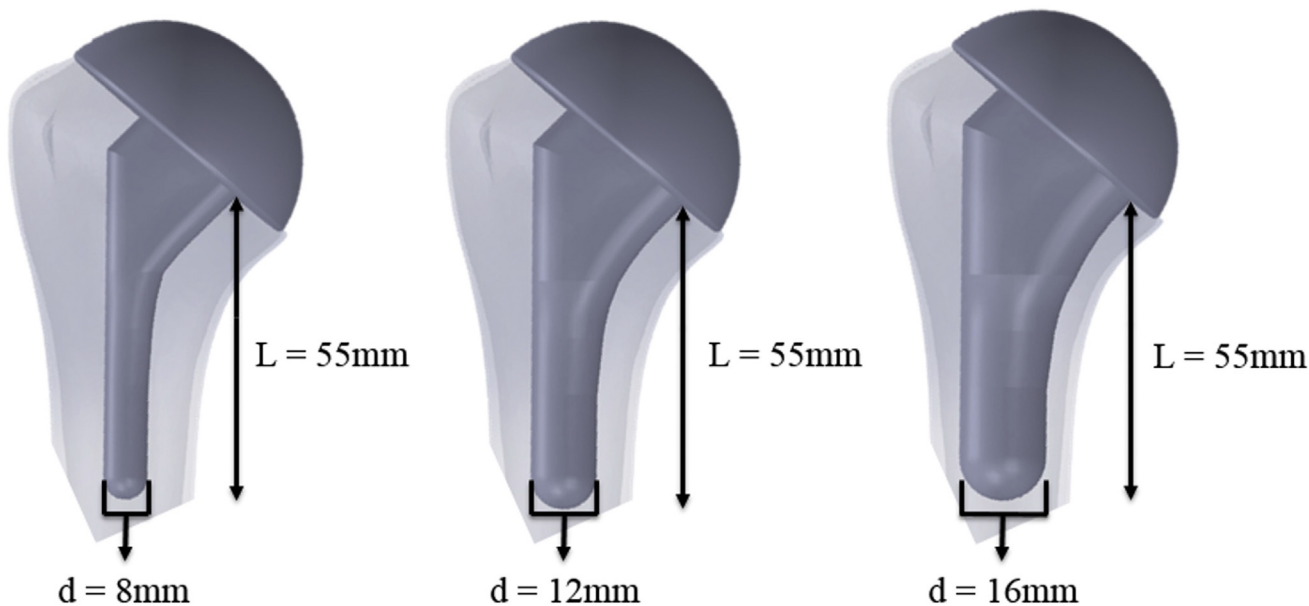
Figure 1 Three generic short-stem implant models were created using SolidWorks CAD software. Implant dimensions were measured from three commercially available humeral implants: Arthrex Univers Apex, Biomet Comprehensive Mini Stem, Wright Medical/Tornier Aequalis Ascend Flex. The shape and *Upper/Middle/Lower* stem dimensions of the three implants were averaged and used to create the generic implant model (*Middle Panel*). This base model was then scaled to create an implant with a thinner (*Left Panel*) diameter and a thicker (*Right Panel*) diameter.
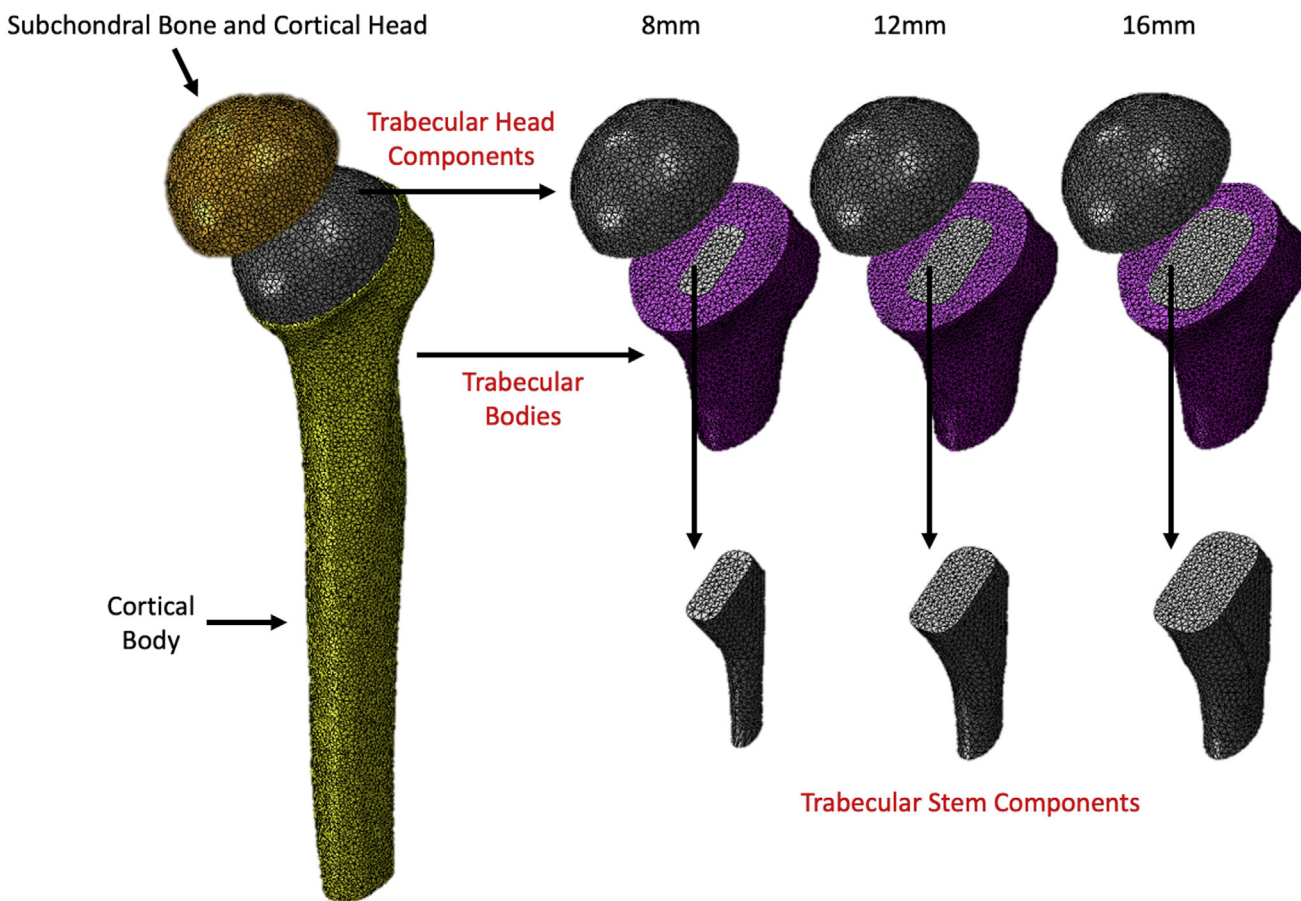

Figure 2 For each humeral implant stem investigated, partitions were created by cutting and reaming the trabecular bone with the desired implant size. These partitions, along with the head components resected in SolidWorks (cortical and trabecular head components), were assembled and merged together maintaining the geometrical lines of the implant allowing for identical mesh generation. Thus, the intact and reconstructed state resulted in identical humeral geometries allowing for direct element-to-element comparison of changes in bone stress.

Bone and implant components were assembled in Abaqus to create 14 FE models (1 intact model + 3 reconstructed models [3 implant sizes] x 2 abduction angles/load directions for each of the 8 specimens used, totaling 64 models. For this experiment, two load directions were investigated that correspond to arm abduction angles of 45° and 75°. Joint reaction forces derived from telemeterized shoulder implant data, assuming 50th percentile male body weight of 88.3 kg, were applied at the articular surface toward the humeral center of rotation with magnitude of 440N and 740N for 45° and 75°, respectively.[2,17] To complete the development of the FE models, the distal ends of the humeri were rigidly fixed to restrict the model in space.

Outcome measures

The amount of BIC, changes in proximal bone stresses from the intact state to the reconstructed state, and changes in SED (used to indicate potential for stress shielding) were determined from the FE simulations. Site-specific averaged values were obtained by dividing the proximal humerus into eight 5-mm-thick slices parallel to the resection surface (Fig. 3). An element was considered to be in a given slice if the centroid of that element fell within the region of that slice.

Bone-to-implant contact

The degree of BIC was calculated using a custom-built LabVIEW code (National Instruments, Austin, TX, USA) by determining the functional contact area (*ie,* contact pressure > 0, where load is being distributed between implant and bone) between the surface elements of the implant to the surrounding bone. If the surface area of an element of interest on the implant had a contact pressure greater than zero, it was considered to be in functional contact with the bone. The surface area of all the elements on the surface of the implant that exhibited a functional contact pressure was summed and then divided by the total surface area of the implant surface elements in the slice of interest to obtain the percentage of BIC.

Proximal bone stress

Changes in stress between the two states (*ie,* reconstructed and intact states) were calculated on an element-by-element basis for both cortical and trabecular bone using a custom code designed in LabVIEW. The six stress components (3 normal and 3 shear) were obtained for each element in the reconstructed and intact states and then subtracted from one another to obtain the von Mises of the change in stress for each element.

Strain energy density

To determine the risk of bone remodeling and volume of bone expected to resorb, the SED for each element was calculated in the reconstructed and intact states on loading, using a custom code designed in LabVIEW.

The capacity of bone resorption was determined using a threshold value of change in SED of 55%, where bone would be expected to remodel and become stronger, remain the same, or resorb if the change in SED was greater than, equal to, or less than this threshold value, respectively.[20] Each element in the slice of interest was placed into one of these three categories depending on its change in SED. To determine the overall percent volume of bone with resorbing potential, the volume of the elements that exhibited change in SED less than the 55% threshold were divided by the sum of the total volume of the elements in all categories.
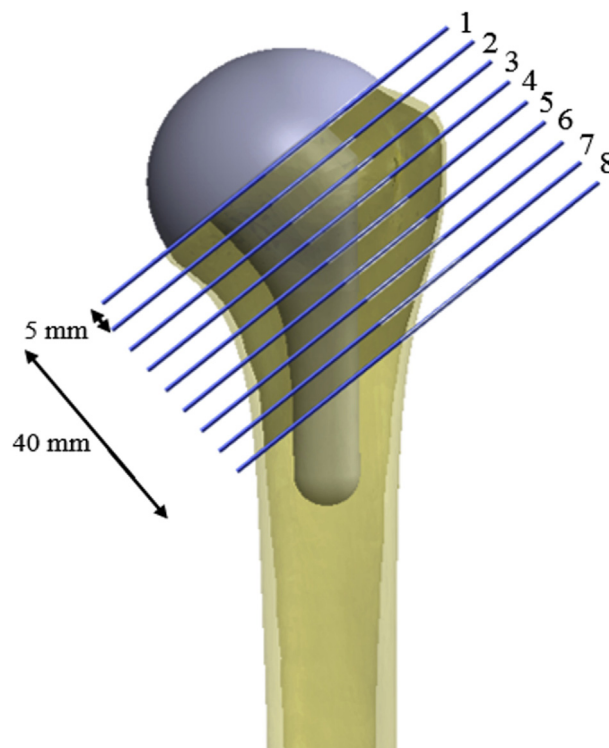

Figure 3 Cortical and trabecular bone were divided into 8 equal 5-mm slices parallel to the resection surface to determine proximal bone stresses and capacity of bone resorption.

Statistical analysis

All three outcome measures were assessed for statistical significance ($\alpha = 0.05$) using a three-way repeated-measures analysis of variance (abduction angle, slice depth, and implant size) using SPSS (IBM, Armonk, NY, USA). Independent variables for the three tests were examined for sphericity and in the event sphericity was rejected, the Greenhouse-Geisser correction was applied.

Results

Sixty-four FE models were created to determine the changes in BIC, proximal bone stresses, and strain energy densities between an intact humeral model and three reconstructed states (distal stem sizes: 8 mm, 12 mm, and 16 mm). Changes in BIC, bone stress, and SED, which are used to determine the capacity of bone resorption, were examined in eight equal slices for both cortical and trabecular bone and are presented in the following sections. Results are presented in terms of abduction angle, which is associated with the direction of load for that specific angle.

Effect of size on BIC

When the three implants were implanted into the humerus models, implant size did not overall significantly affect the degree of BIC (45°: $P = .080$; 75° $P = .076$). However, when BIC was analyzed at each individual slice depth, statistically significant differences were identified ($P < .001$, power = 1.0 for both abduction angles) (Fig. 4). At 45° of abduction and for all slice depths investigated, increasing implant cross-section from thin to medium and increasing from medium to thick had no significant effect on BIC (percent change in contact = 0.9 ± 0.3%, $P = .3$ and 5.6 ± 1.1%,
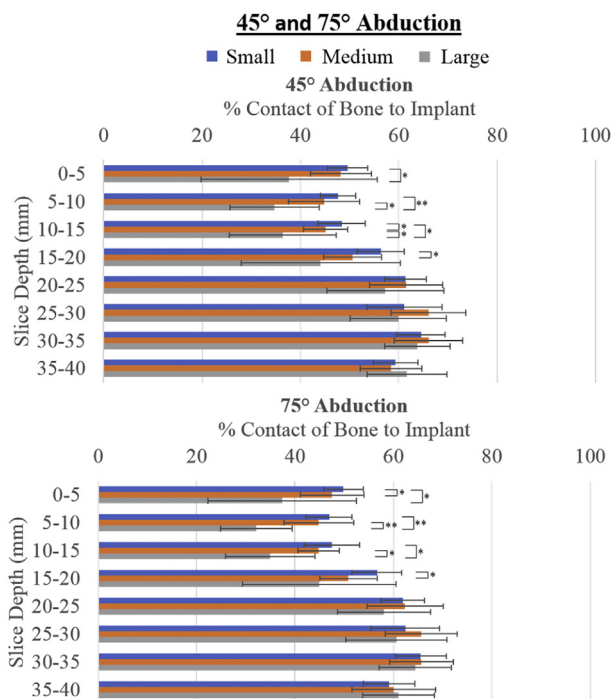
45° and 75° Abduction

Figure 4 The percent contact of the humeral implant to bone at 45° and 75° of abduction. Statistically significant difference is expressed with *$P \leq .05$ and **$P \leq .001$.

$P = .07$, respectively). Examining each slice depth individually, the implant that resulted in the greatest amount of contact changed depending on slice. The thin implant produced the greatest amount of contact in the first 4 slices, the medium produced the most contact in slices 5-7, and the thick implant produced the greatest amount of contact in the most distal slice (Fig. 4). Statistically significant changes in degree of contact were only observed in the first four slices.

Effect of size on proximal bone stress

Several statistically significant changes in bone stress were found throughout the 8 slices for cortical and trabecular bone for both 45° and 75° articular loading scenarios (Fig. 5).

Cortical bone stresses

At abduction angles of 45° and 75°, both implant size ($P < .001$, power = 1.0) and slice depth ($P < .001$, power = 1.0) had statistically significant effects on change in cortical bone stress compared to the intact state. At 45° of abduction and for all slice depths investigated, increasing implant size from thin to medium increased the average change in bone stress by $3.2 \pm 0.2\%$ ($P = .002$) and increasing the implant size from medium to thicker increased the average change in bone stress by $10.4 \pm 0.6\%$ ($P < .001$). The thin implant consistently produced the smallest changes in stress compared with the intact state.

Trabecular bone stress

Statistically significant changes in trabecular bone stress when compared with the intact state were observed at abduction angles of 45° and 75° for both implant size ($P < .001$, power = 1.0) and slice depth ($P < .001$, power = 1.0). For all slice depths investigated at 45° abduction, increasing implant size caused bone stresses to increase

by an average of $3.8 \pm 2\%$ ($P < .001$) and $10.9 \pm 0.6\%$ ($P < .001$) for the thinner to medium and medium to thicker implants, respectively. Average changes in bone stress for all slices when the arm was abducted 75° increased by $4.2 \pm 0.2\%$ ($P < .001$) and $12.0 \pm 0.6\%$ ($P < .001$) for the thinner to medium and medium to thicker implant sizes, respectively. The smallest implant size resulted in the smallest percent change in trabecular bone stress for all slices, except for the most proximal slice, where the largest implant was found to more closely represent the intact state.

Effect of implant size on the risk of bone resorption

Several significant changes in the SED outcome were found throughout the 8 slices when increasing implant size in both cortical and trabecular bone when the arm was loaded at 45° and 75° of abduction (Fig. 6). The results are divided into the following sections: cortical bone resorbing potential and trabecular bone resorbing potential. The change in SED is proposed to be directly related to the risk of bone resorption; thus, results are presented in terms of percent of bone volume with potential to resorb.

Cortical bone: For abduction angles of 45° and 75°, implant size ($P = .002$, power$\geq$0.9) and slice depth ($P < .001$, power = 1.0) had statistically significant effects on the change in SED and thus the percent volume of bone with resorbing potential. For both abduction angles, the smallest implant size consistently produced the lowest volume of bone with resorbing potential when compared with the larger sizes. At 45° of abduction and for all slices depths investigated, increasing implant size from thinner to medium increased the overall percent volume of bone with resorbing potential by $3.8 \pm 0.3\%$ ($P = .002$) and increasing the implant size from medium to thick increased the average volume by $16.2 \pm 1.3\%$ ($P = .004$). In all slice depths, the thinner implant size consistently produced the lowest volume with resorption potential. At 75° abduction and for all slice depths investigated, the overall bone volume with resorbing potential increased by $4.3 \pm 0.4\%$ ($P = .008$) and $17.5 \pm 1.4\%$ ($P = .003$) when increasing the implant size from thin to medium and medium to thick, respectively. Similar to 45° abduction, the smallest implant size presented the lowest volume of bone with resorbing potential in all slice depths. In addition, when assessing the location of potential bone resorption, higher levels of bone resorbing potential occurred proximally in the humerus as compared with distally.

Trabecular bone: For all abduction angles, both implant size (45°: abduction $P = .01$, power = 0.8; 75° abduction: $P = .01$, power = 0.8) and slice depth (45° and 75° abduction: $P \leq .001$, power$\geq$0.9) significantly affected the volume of trabecular bone with the potential to resorb. For both abduction angles, the thinner implant was most consistent in producing the lowest volume of bone with resorbing potential in all slice depths when compared with the other implant sizes.

Discussion

Short-stem and stemless implants have been introduced in an attempt to limit stress shielding and the amount of trabecular and cortical bone that is compromised during shoulder arthroplasty. Recent clinical literature, however, has reported the presence of stress shielding and bone resorption in some short-stem implants.[8,21] The results of this computational FE modeling study support the clinical literature, that stress shielding occurs in shorter-stem implants. In addition, our data demonstrated that selection of a thinner implant with a lower canal fill ratio resulted in substantially lower alterations in bone stresses from the intact state. These thinner humeral implants also resulted in a substantially lower volume of bone with stress shielding and resorption
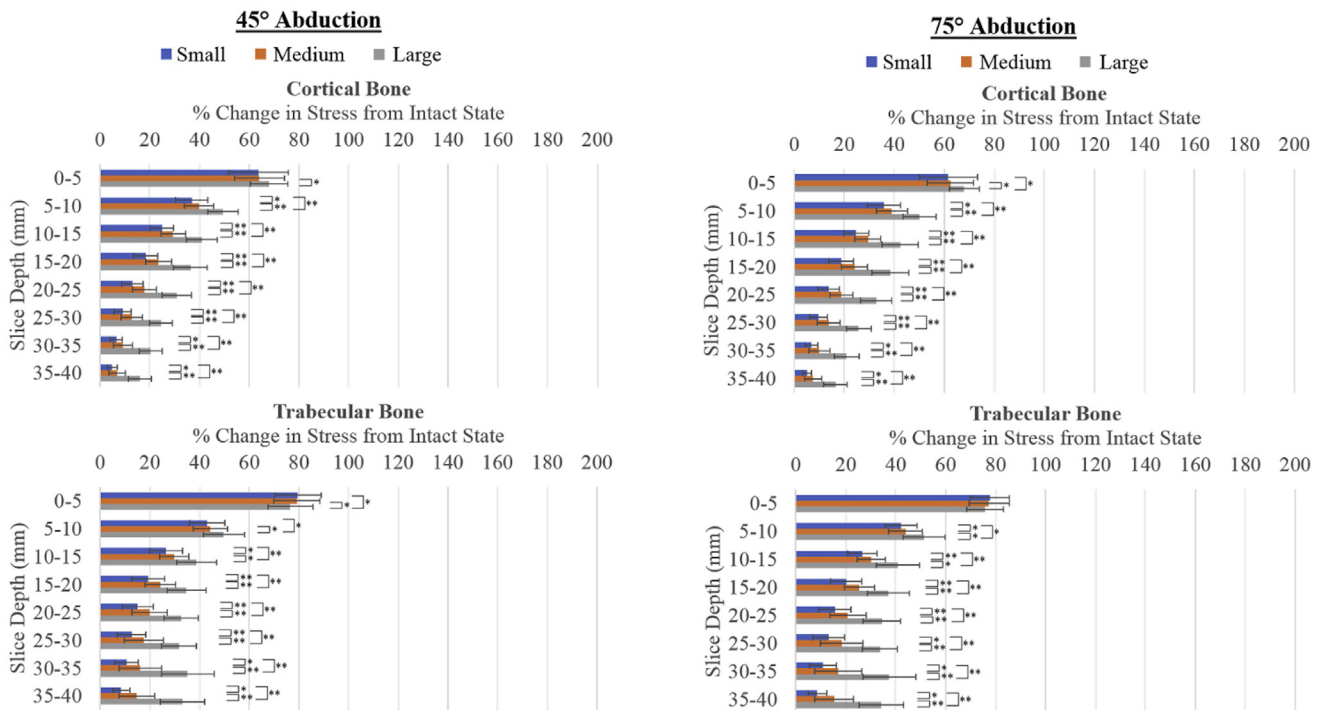
Figure 5 Changes in proximal bone stress when implant size, and therefore canal fill ratio, were increased at 45° (*Left Panel*) and 75° (*Right Panel*) of abduction. Statistically significant difference is expressed with *$P \leq$ .05 and **$P \leq$ .001 (Note: the more favorable outcome for this variable is 0% change in stress from the intact state).
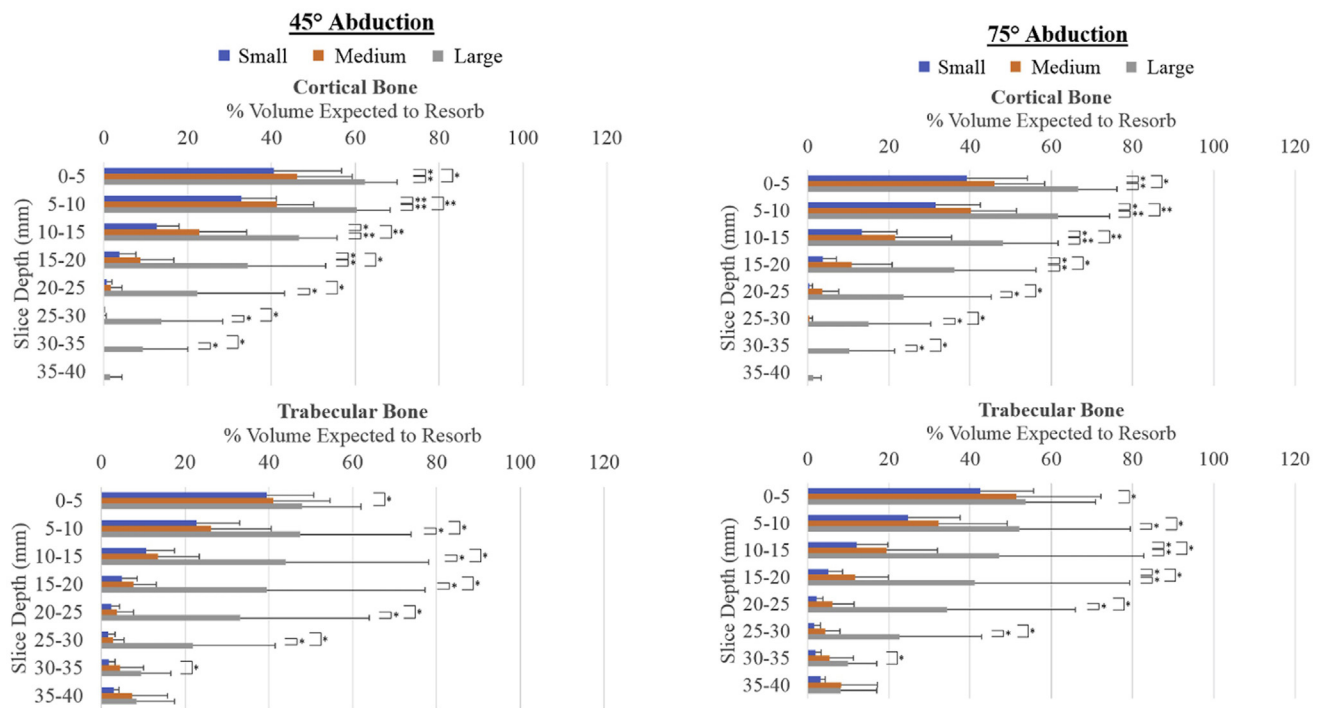

Figure 6 The percentage of proximal humerus bone volume with resorbing potential when implant size, and therefore canal fill ratio, was increased at 45° at 75° of abduction. Statistically significant difference is expressed with *$P \leq$ .05 and **$P \leq$ .00. (Note: the more favorable outcome for this variable is 0% volume of bone resorption).

potential when compared with the medium and thicker stems. Raiss et al[21] recommended a canal fill ratio of less than 0.7 based on a clinical evaluation of follow-up radiographs of a curved short-stem implant. This computational study scientifically supports the findings of Raiss et al, as the volume of bone expected to resorb

increased 2%-4% when the canal fill ratio increased from 0.4 to 0.6, and when the canal fill ratio increased to 0.8, the volume of bone expected to resorb substantially increased to 16%-18%.

The current work also agrees with the work of Langohr et al[16] who investigated a single commercially available short-stem

humeral implant. The authors reported for trabecular bone that with a larger implant, there were corresponding increases in the proportion of bone with resorbing potential, ranging from 1.1% to 5.5 % depending on anatomical quadrant and depth from the resection plane. The importance of the conclusions of the present study is that these resulting trends may be applied more generically, as the tested humeral stem was created as an average of three commercially available short-stem implants.

When humeral implant size was increased, statistically significant changes in bone stress were observed throughout all slices for cortical and trabecular bone at both abduction angles, except the most proximal trabecular bone slice at 75° abduction. On a per slice basis, the thinner implant was almost always more consistent at mimicking cortical and trabecular bone stresses in the intact state. According to Huiskes,[13,14] when an implant is placed into bone, the load applied to the joint is no longer transferred solely through the cortical shell and metaphyseal trabecular bone but now involves the interface between the bone and implant. The load applied to the articular surface is now shared across the bone and implant,[10,13] resulting in subnormal bone stresses when compared with the native loading state.[13] It is thus logical to conclude that when an implant with a relatively larger size is implanted into bone, more of the load from the articular surface is accepted by the larger stem when compared with implants with a smaller size. As the larger stem accepts more of the applied load, less is shared to the surrounding cortical and trabecular bone over the entire length of the implant. When an implant with a smaller size is inserted into the bone, there is a greater percentage of the load being shared to the bone; thus, better matching stress distributions in the native loading state. This theory is supported by the changes in bone stress observed in the present investigation.

In the most proximal trabecular bone slice, the larger implant better matched native bone stresses. This likely occurred because of the larger implant's closer proximity to the cortical bone. Having the larger implant contact the peripheral cortical bone results in a similar load transmission as in the native state, when the subchondral bone transmits loads radially to the peripheral cortical bone at the humeral neck.[22,29] The results suggest that the implant with the largest cross section may be sharing more of the load in the most proximal slice with the cortical shell that would otherwise be shared with trabecular bone when a smaller implant was used, thus better representing the load distribution in trabecular bone as seen in the native state. These findings of thicker/larger implant shape at the most proximal aspect of the humeral neck osteotomy resulting in more normalized stress may support the use of an implant collar or trunnion.

Statistically significant changes in the percentage of cortical bone volume with resorbing potential were observed within the proximal humerus owing to increasing implant size. The findings of this experiment show that the thinner implant size was most consistent at producing the smallest amount of bone volume with the potential to resorb when compared to the medium and thick sizes in all depths. Stress shielding with the thinner implant, however, was only found in the proximal 5 slices, where significantly lower bone volumes with resorbing potential were noted when compared with the other two implant sizes. Thus, it is recommended that an implant with a smaller diameter should be used over larger sizes, providing acceptable time zero fixation can be achieved, to decrease the overall risk of proximal cortical bone stress shielding. Trabecular bone changes were also observed across all abduction angles and various slice depths. For all abduction angles, increasing implant size significantly affected the volume of trabecular bone that had the potential to resorb.

The findings of this computational study agree with previously published clinical studies, suggesting that larger stem diameters lead to increased occurrences of cortical stress shielding.[4,9,19] One study, investigating relative implant size in the humerus, found that patients who received a shoulder replacement with a larger relative stem diameter, which resulted in greater incidences of cortical stress shielding particularly on the proximal-lateral aspect.[19] Studies investigating stress shielding in the hip found that larger stem diameters ($\geq$13.5 mm), when compared with smaller stem diameters ($\leq$12.0 mm), resulted in greater incidences (approximately 44% greater) of pronounced cortical bone resorption.[4,9]

The strength of this computational study is that it agrees with previous clinical studies and validates the mechanics of load transmission and stress shielding. This is important, as it demonstrates future implant design projects may benefit from computational finite element modeling to optimize stem geometry and sizing. In addition, the use of preoperative surgical planning software is becoming more common. The addition of basic modeling to these programs may allow the optimization of humeral stem sizing to minimize the potential for stress shielding and bone resorption. Finally, the generic implant created and tested in this study was an average of three commercially available short-stem designs, as such, the findings of this study may be more generalizable to clinically used arthroplasty systems.

The limitations of this study included that only one average implant shape was studied. In addition, only limited loading orientations were examined, as such, the effects of active internal and external rotation may be different. In addition, many patient's postarthroplasty return to strenuous recreational and occupational tasks and the increased load of these activities on stress shielding were not examined.

Conclusion

The aim of this study was to provide insight on the degree of BIC, changes in bone stresses from the intact state, and changes in strain energy density, which can be used to predict stress shielding and the volume of bone with resorbing potential. Our findings indicate that BIC did not substantially differ between the ranges of stem sizes tested. The thinner stem with the lowest canal fill ratio, however, did produce significantly lower changes in cortical and trabecular bone stresses from the intact state. In addition, the thinnest humeral implant also resulted in the lowest volume of cortical and trabecular bone with resorbing potential when compared with the medium and thicker implants. In summary, providing time-zero sufficient humeral implant fixation is attained, selection of a thinner diameter humeral stem results in a better stress profile and the lower volume of bone with resorbing potential owing to stress shielding.

Disclaimers:

References

1. Behrens BA, Bouguecha A, Nolte I, Meyer-Lindenberg A, Stukenborg-Colsman C, Pressel T. Strain adaptive bone remodelling: influence of the implantation technique. Stud Health Technol Inform 2008;133:33-44.

2. Bergmann G, Graichen F, Bender A, Kääb M, Rohlmann A, Westerhoff P. In vivo glenohumeral contact forces–measurements in the first patient 7 months postoperatively. J Biomech 2007;40:2139-49. https://doi.org/10.1016/j.jbiomech.2006.10.037.

3. Bilhan H, Geckili O, Mumcu E, Bozdag E, Sünbüloğlu E, Kutay O. Influence of surgical technique, implant shape and diameter on the primary stability in cancellous bone. J Oral Rehabil 2010;37:900-7. https://doi.org/10.1111/j.1365-2842.2010.02117.x.

4. Bobyn JD, Mortimer ES, Glassman AH, Engh CA, Miller JE, Brooks CE. Producing and avoiding stress shielding. Laboratory and clinical observations of non-cemented total hip arthroplasty. Clin Orthop Relat Res 1992;274:79-96.

5. Casagrande DJ, Parks DL, Torngren T, Schrumpf MA, Harmsen SM, Norris TR, et al. Radiographic evaluation of short-stem press-fit total shoulder arthroplasty: short-term follow-up. J Shoulder Elbow Surg 2016;25:1163-9. https://doi.org/10.1016/j.jse.2015.11.067.

6. Collin P, Matsukawa T, Boileau P, Brunner U, Walch G. Is the humeral stem useful in anatomic total shoulder arthroplasty? Int Orthop 2017;41:1035-9. https://doi.org/10.1007/s00264-016-3371-4.

7. Denard PJ, Noyes MP, Walker JB, Shishani Y, Gobezie R, Romeo AA, et al. Proximal stress shielding is decreased with a short stem compared with a traditional-length stem in total shoulder arthroplasty. J Shoulder Elbow Surg 2018;27:53-8. https://doi.org/10.1016/j.jse.2017.06.042.

8. Denard PJ, Noyes MP, Walker JB, Shishani Y, Gobezie R, Romeo AA, et al. Radiographic changes differ between two different short press-fit humeral stem designs in total shoulder arthroplasty. J Shoulder Elbow Surg 2018;27:217-23. https://doi.org/10.1016/j.jse.2017.08.010.

9. Engh CA, Bobyn JD. The influence of stem size and extent of porous coating on femoral bone resorption after primary cementless total hip arthroplasty. Clin Orthop Relat Res 1988;231:7-28.

10. Frost HM. A 2003 Update of bone physiology and Wolff's Law for clinicians. Angle Orthod 2004;74:3-15. https://doi.org/10.1043/0003-3219(2004)074<0003:AUOBPA>2.0.CO;2.

11. Gefen A. Computational simulations of stress shielding and bone resorption around existing and computer-designed orthopaedic screws. Med Biol Eng Comput 2002;40:311-22. https://doi.org/10.1007/BF02344213.

12. Haase K, Rouhi G. Prediction of stress shielding around an orthopedic screw: using stress and strain energy density as mechanical stimuli. Comput Biol Med 2013;43:1748-57. https://doi.org/10.1016/j.compbiomed.2013.07.032.

13. Huiskes R. Stress shielding and bone resorption in THA: clinical versus computer-simulation studies. Acta Orthop Belg 1993;59:118-29.

14. Huiskes R, Weinans H, Grootenboer HJ, Dalstra M, Fudala B, Slooff TJ. Adaptive bone-remodeling theory applied to prosthetic-design analysis. J Biomech 1987;20:1135-50.

15. Keener JD, Chalmers PN, Yamaguchi K. The humeral implant in shoulder arthroplasty. J Am Acad Orthop Surg 2017;25:427-38. https://doi.org/10.5435/JAAOS-D-15-00682.

16. Langohr GDG, Reeves J, Roche CP, Faber KJ, Johnson JA. The effect of short stem humeral component sizing on humeral bone stress. J Shoulder Elbow Surg 2020;29:761-7. https://doi.org/10.1016/j.jse.2019.08.018.

17. McDowell MA, Fryar CD, Ogden CL, Flegal KM. Anthropometric reference data for children and adults: United States, 2003-2006. Natl Health Stat Rep 2008;10:1-48.

18. Morgan EF, Bayraktar HH, Keaveny TM. Trabecular bone modulus-density relationships depend on anatomic site. J Biomech 2003;36:897-904. https://doi.org/10.1016/s0021-9290(03)00071-x.

19. Nagels J, Stokdijk M, Rozing PM. Stress shielding and bone resorption in shoulder arthroplasty. J Shoulder Elbow Surg 2003;12:35-9. https://doi.org/10.1067/mse.2003.22.

20. Neuert MA, Dunning CE. Determination of remodeling parameters for a strain-adaptive finite element model of the distal ulna. Proc Inst Mech Eng H 2013;227:994-1001. https://doi.org/10.1177/0954411913487841.

21. Raiss P, Schnetzke M, Wittmann T, Kilian CM, Edwards TB, Denard PJ, et al. Postoperative radiographic findings of an uncemented convertible short stem for anatomic and reverse shoulder arthroplasty. J Shoulder Elbow Surg 2019;28:715-23. https://doi.org/10.1016/j.jse.2018.08.037.

22. Razfar N, Reeves JM, Langohr DG, Willing R, Athwal GS, Johnson JA. Comparison of proximal humeral bone stresses between stemless, short stem, and standard stem length: a finite element analysis. J Shoulder Elbow Surg 2016;25:1076-83. https://doi.org/10.1016/j.jse.2015.11.011.

23. Reeves JM, Johnson JA, Athwal GS. An analysis of proximal humerus morphology with special interest in stemless shoulder arthroplasty. J Shoulder Elbow Surg 2018;27:650-8. https://doi.org/10.1016/j.jse.2017.10.029.

24. Schnetzke M, Coda S, Raiss P, Walch G, Loew M. Radiologic bone adaptations on a cementless short-stem shoulder prosthesis. J Shoulder Elbow Surg 2016;25:650-7. https://doi.org/10.1016/j.jse.2015.08.044.

25. Shishani Y, Gobezie R. Does a short-stemmed humeral implant really make a difference? Semin Arthroplasty 2017;28:13-7. https://doi.org/10.1053/j.sart.2017.05.003.

26. Tissakht M, Ahmed AM, Chan KC. Calculated stress-shielding in the distal femur after total knee replacement corresponds to the reported location of bone loss. J Orthop Res 1996;14:778-85.

27. Van Lenthe GH, de Waal Malefijt MC, Huiskes R. Stress shielding after total knee replacement may cause bone resorption in the distal femur. J Bone Joint Surg Br 1997;79:117-22.

28. Wagner ER, Statz JM, Houdek MT, Cofield RH, Sánchez-Sotelo J, Sperling JW. Use of a shorter humeral stem in revision reverse shoulder arthroplasty. J Shoulder Elbow Surg 2017;26:1454-61. https://doi.org/10.1016/j.jse.2017.01.016.

29. Wang Y, Li J, Yang J, Dong J. Regional variations of cortical bone in the humeral head region: a preliminary study. Bone 2018;110:194-8. https://doi.org/10.1016/j.bone.2018.02.010.

30. Willing RT, Lalone EA, Shannon H, Johnson JA, King GJW. Validation of a finite element model of the human elbow for determining cartilage contact mechanics. J Biomech 2013;46:1767-71. https://doi.org/10.1016/j.jbiomech.2013.04.001.